

# Continuous-wave laser-induced glass fiber generation

Nobuyasu Nishioka<sup>1</sup> · Hirofumi Hidai<sup>1</sup>  · Souta Matsusaka<sup>1</sup> · Akira Chiba<sup>1</sup> · Noboru Morita<sup>1</sup>

Received: 23 May 2017 / Accepted: 19 August 2017 / Published online: 29 August 2017  
© Springer-Verlag GmbH Germany 2017

**Abstract** Pulsed-laser-induced glass fiber generation has been reported. We demonstrate a novel glass fiber generation technique by continuous-wave laser illumination and reveal the generation mechanism. In this technique, borosilicate glass, metal foil, and a heat insulator are stacked and clamped by a jig as the sample. Glass fibers are ejected from the side surface of the borosilicate glass by laser illumination of the sample from the borosilicate glass side. SEM observation shows that nanoparticles are attached on the glass fibers. High-speed imaging reveals that small bubbles are formed at the side surface of the borosilicate glass and the bursting of the bubble ejects the fibers. The temperature at the fiber ejection point is estimated to be  $\sim 1220$  K. The mechanism of the fiber ejection includes the following steps: the metal thin foil heated by the laser increases the temperature of the surrounding glass by heat conduction. Since the absorption coefficient of the glass is increased by increasing the temperature, the glass starts to absorb the laser irradiation. The heated glass softens and bubbles form. When the bubble bursts, molten glass and gas inside the bubble scatter into the air to generate the glass fibers.

## 1 Introduction

Glass fibers are classified into glass wool or glass fibers, depending on the length, and a long fiber is called a glass fiber. The high tensile strength and corrosion resistance of a

glass fiber are exploited for glass fiber reinforced plastic (GFRP). GFRP is used in the body of ships [1], aircrafts [2], and to reinforce concrete beams [3]. Although normal glass fiber is an insulator, a conductive highly durable glass fiber is achieved by adding carbon black to the glass fiber. The conductive glass fiber is expected to be used in aircrafts or electrical devices [4]. In industrial glass fiber production, glass is heated to approximately 1900 K and softened in a tank furnace. Then, the softened glass is placed in a spinning furnace and the glass fiber is spun. This method is called the direct melt method [5].

Fiber generation by laser illumination of various substrates has been reported. Femtosecond laser illumination (wavelength: 515 nm) of substrates such as graphite, lead, aluminum, and tin forms fibrous nanoparticles [6]. Nanosecond ultra-violet (UV) laser illumination of a polymer substrate generates fibers [7]. Nanosecond laser (wavelength: 355 nm) [8] and femtosecond laser (wavelength: 1030 nm) [9, 10] illumination of glass generate glass fibers with diameters in the order of  $\sim 100$  nm. Focused femtosecond laser illumination achieves a high peak power density, causes multi-photon absorption, and generates glass fibers. The glass fibers are generated in the direction parallel to the optical axis. Additionally, microsecond CO<sub>2</sub> laser (wavelength: 10.6  $\mu$ m) illumination of a glass substrate causes a filamentary melt-ejection from the surface of the glass substrate [11]. In the glass fiber generation, the temperature has not been determined, even though the temperature is an essential parameter as the viscosity of glass decreases as the temperature increases [12].

Glass machining with a near infrared (IR) continuous-wave (CW) laser beam (wavelength: 1064 nm) is difficult, because the absorptivity of glass for the laser irradiation is low. The authors have reported a modification method of

✉ Hirofumi Hidai  
hidai@faculty.chiba-u.jp

<sup>1</sup> Department of Mechanical Engineering, Chiba University, Chiba, Japan

glass called CW laser backside irradiation (CW-LBI) [13–16]. In CW-LBI, the glass is modified with a laser beam. The modification mechanism is explained as follows. The sample is stacked in the order of borosilicate glass, metal foil, and heat insulator, and clamped with a jig and the laser is illuminated from the side of the glass. The glass is transparent to the laser beam. The metal foil absorbs the laser irradiation and is heated. The heated metal foil heats the peripheral glass and the glass starts to absorb the laser, because the absorptivity of the glass increases with increasing temperature. The peripheral glass around the heated glass is also heated and the heat spot moves toward the light source. The trajectory of the heat spot migration is modified because of the rapid heating and quenching. A similar phenomenon, named fiber fuse, occurs in the optical fiber when the fiber transmits a high power laser.

We observed that glass fibers with a diameter in the order of 100 nm were ejected from the side surface of borosilicate glass during the CW-LBI experiment. In this paper, we demonstrate a novel technique to generate glass fibers with CW-LBI. Scanning electron microscopy (SEM) images revealed the microstructure. High-speed imaging clarified the glass fiber generation process where the glass fibers were ejected from the side surface of the glass into the air. In addition, the temperature distribution of the glass was indispensable to elucidate the mechanism; hence, the temperature field of the sample was measured.

## 2 Experimental methods

Figure 1 shows the schematic illustration of the experimental apparatus. Figure 1a–c shows the overall view, top view along the  $y$ -axis and side view along the  $x$ -axis, respectively. The laser illumination, at a scan rate of  $50 \mu\text{m/s}$ , to the area of a depth of  $\sim 1 \text{ mm}$  from the surface to the surface emitted the glass fiber. The laser oscillator (RFL-C020/A/2/A, Wuhan Raycus Fiber Laser Technologies Co., Ltd., Hubei, China) emits CW irradiation with a wavelength of 1064 nm. The power was set at 18.6 W.

The sample consisted of borosilicate glass (Pyrex<sup>®</sup>, Corning 7740, Corning Inc., NY, USA), metal foil (stainless steel, SUS304 foil, #753173, Nilaco Corp. Tokyo, Japan) and silica glass. The borosilicate glass was the source of the fiber and the silica glass was the heat insulator. The size of the borosilicate glass and the silica glass was  $20 \text{ mm} \times 20 \text{ mm} \times 5 \text{ mm}$ . The thickness of the metal foil was 0.01 mm. The sample was stacked and clamped with a jig in the order of borosilicate glass, metal foil and silica glass from the laser oscillator side. The metal foil absorbed the laser irradiation and was heated because the laser light was transmitted through the borosilicate glass at

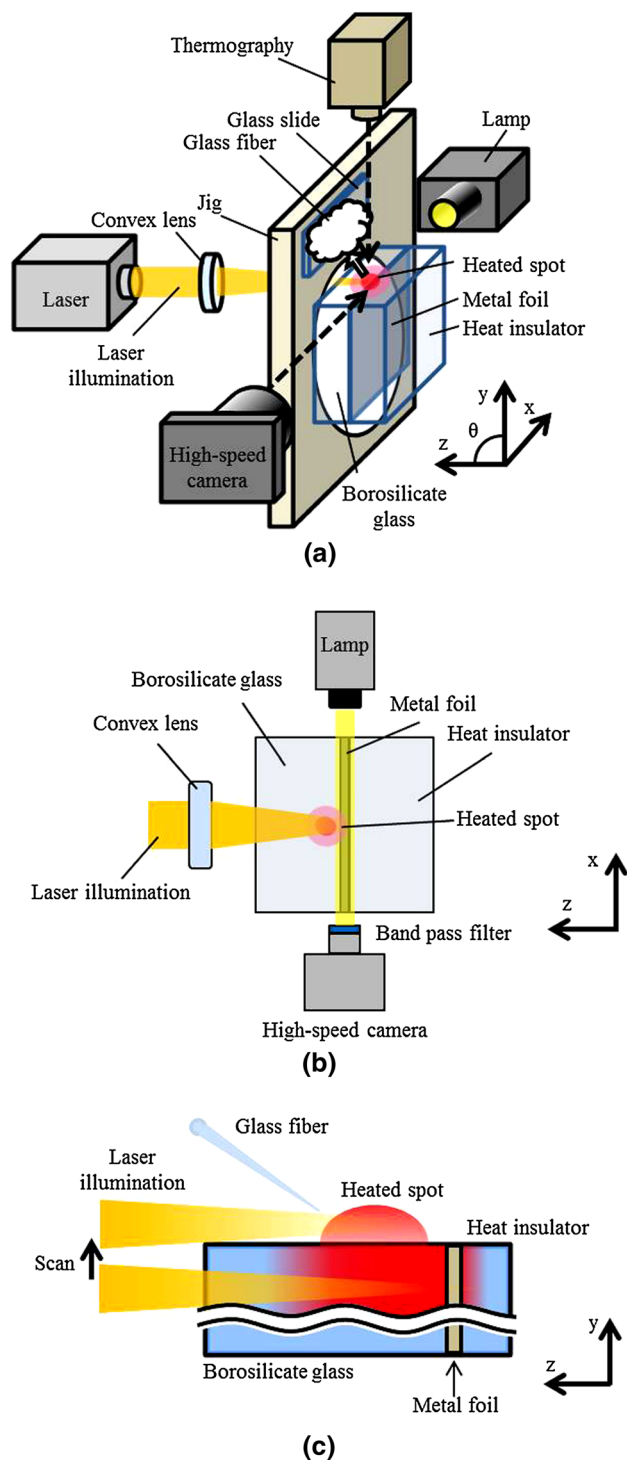


**Fig. 1** Schematic illustration of the experimental apparatus. **a** The overall view and **b** top view in the  $y$ -axis direction. **c** Side view in the  $x$ -axis direction

normal temperature. The heated metal foil heated the peripheral glass. The spot diameter at the metal foil and the fiber forming point was approximately 245 and 200  $\mu\text{m}$ , respectively. Glass fibers were ejected into the air and

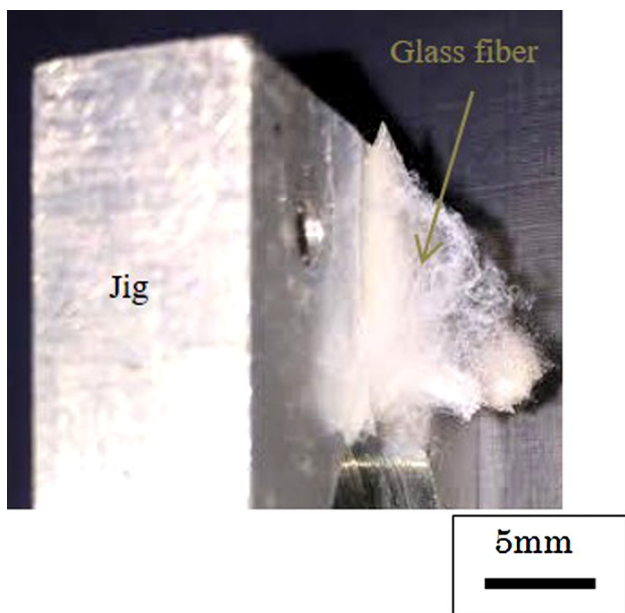


Fig. 2 A photo of the glass fibers deposited on a jig

adhered to the back surface of the jig. For SEM, a glass slide was placed on the back surface of the jig and the fibers were deposited on the slide as shown in Fig. 1a.

The fibers ejected from the borosilicate glass into the air were observed using a high-speed camera (Phantom V7.3, Vision Research Inc., NJ, USA). The frame rate of the high-speed camera was set at 10,000 frames per second. The setup of the camera and illumination light (LS-M250, Sumita Optical Glass, Inc., Saitama, Japan) is shown in Fig. 1. The transmitted light image was observed by placing the illumination light on the other side of the high-speed camera. Thermal radiation from the heated borosilicate glass prevented the observation of the fiber ejection regime. To filter the radiation, a band-pass filter (10BPF10-440, Newport Corp., Irvine, CA, USA) was placed between the camera and the sample.

Thermography (TVS-620, Nippon Avionics Co., Ltd., Tokyo, Japan) revealed the temperature distribution of the spot where the fibers were ejected and detected infrared light with a wavelength of 8–16  $\mu\text{m}$ . Therefore, the

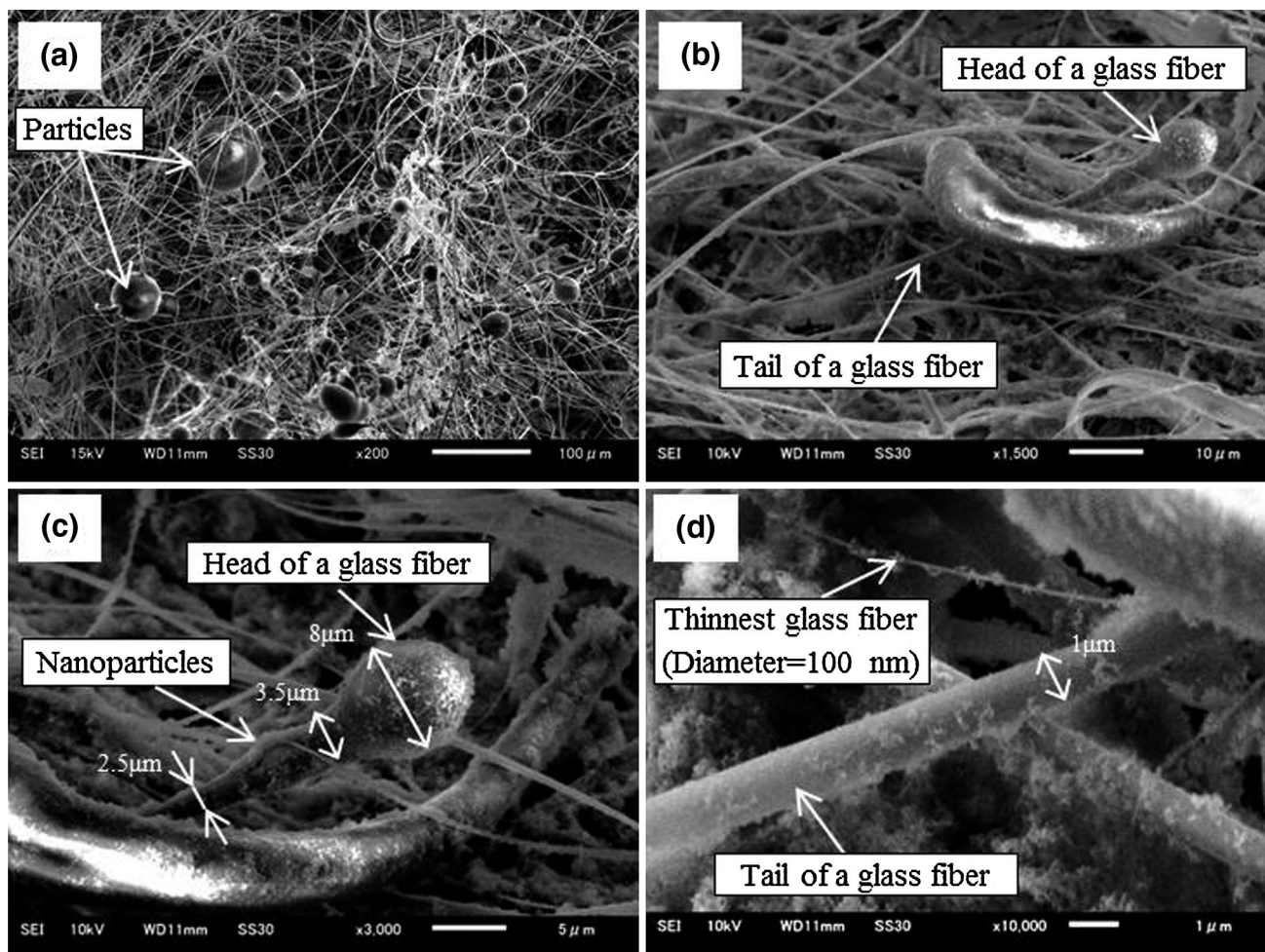


Fig. 3 SEM micrographs of the glass fibers

scattered laser beam did not affect the temperature estimation. The maximum measurable temperature was 1173 K. The temperature on the top surface of the glass was measured. The emissivity of the borosilicate glass was necessary to determine the temperature of the glass. The emissivity has been reported to be 0.86 at 735 K [17]. However, the emissivity depends on the surface shape and the sample temperature; hence, the emissivity was determined under our experimental conditions. The emissivity at the temperature where the fibers were ejected was required. The borosilicate glass embedded with a thermocouple was heated to 752 K using a heater, and the emissivity was estimated by matching the temperature obtained by thermography and the thermocouple at 752 K. As a result, the emissivity was calculated to be 0.94 at 752 K. The temperature was believed to be higher than the softening point

(1094 K); however, the heater was unable to heat the glass over 752 K in an air atmosphere. Therefore, the emissivity was determined at 752 K.

### 3 Results and discussion

Figure 2 shows the glass fibers deposited on the jig. To observe the fibers with SEM, glass fibers were deposited on the glass slide that was attached on the jig. The glass fibers were mainly ejected into the air at an angle of  $\theta = 30\text{--}60^\circ$ . The angle  $\theta$  was defined as the angle from the z-axis to y-axis, as shown in Fig. 1a. Figure 3 shows the SEM images of the glass fiber deposited on the glass slide. Figure 3a shows the glass fibers. Fibrous and spherical parts were observed, and the diameters of the spherical parts were

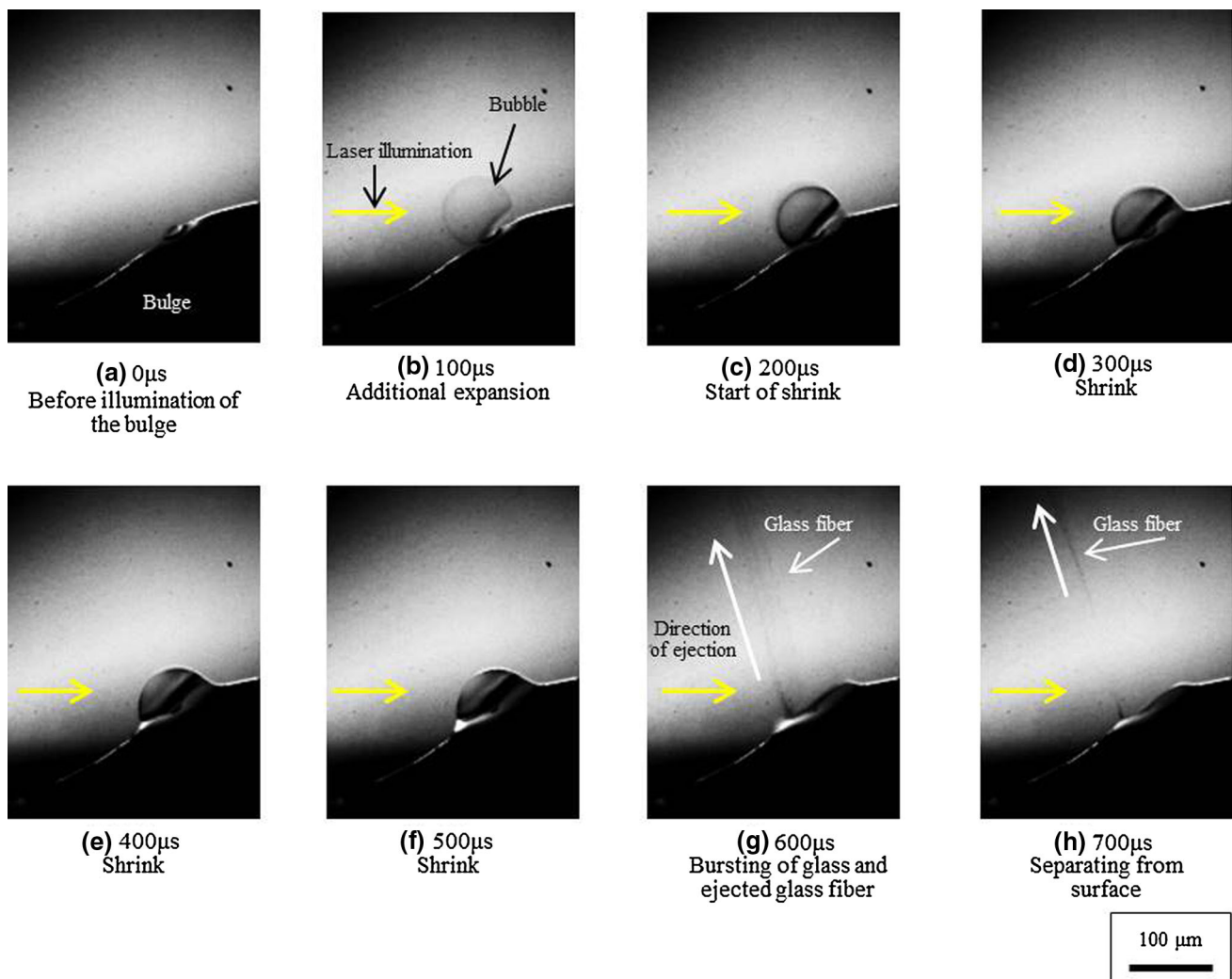


**Fig. 4** Time lapse images of the fiber. Laser illumination of the sample heated the glass and the vicinity of the upper surface of the bulged sample (a). Scanning the laser beam to the bulge caused

additional expansion, bubble (b). The bubble shrinks (c–f), bursts to eject a glass fiber into the air (g) and separates from the surface of the sample (h)

dispersed. The typical shape of a glass fiber was tadpole like as shown in Fig. 3b. The head part was inflated to be spherical and the diameter became thinner from the head to the tail. Figure 3c shows an enlarged view of the head of the glass fiber, where the shape of the head was elliptical with a diameter of  $\sim 8 \mu\text{m}$ . The diameter became thinner from  $8 \mu\text{m}$  at the top to  $2.5 \mu\text{m}$  at the tail, as indicated in Fig. 3c. Additionally, nanoparticles with a diameter of  $\sim 100 \text{ nm}$  were attached on the glass fiber. Figure 3d shows the enlarged image of the fiber tail; the diameter was  $\sim 1 \mu\text{m}$  and constant. The diameter depended on each fiber, and the thinnest observed fiber had a diameter of  $\sim 100 \text{ nm}$ . Additionally, nanoparticles were attached to the tail in the same manner as at the head.

Figure 4 shows time lapse images of the fiber ejection obtained using a high-speed camera. Laser illumination to the vicinity of the upper surface of the sample heated the stainless steel foil and softened the vicinity of the glass, and then the upper surface of the borosilicate glass became bulged. In Fig. 4a, the part of the upper surface expansion at the borosilicate glass is referred to as the bulge. Scanning the laser beam from the original borosilicate glass to the bulge along the y-axis caused an additional expansion (as shown in Fig. 4b). The additional expansion is referred to as the bubble. As shown in Fig. 4c–f, the bubble gradually shrank. The bubble bursts and the glass fiber was ejected into the air (as shown in Fig. 4g)  $600 \mu\text{s}$  after laser illumination of the upper surface. Figure 4h shows the separation of the fiber from the surface.

The temperature of the fiber ejected area at which the fibers were being emitted, after the bulge was generated by scanning the laser, was measured by thermography. The fibers were emitted from the bulge continuously by laser illumination of the bulge. Figure 5 shows the top view temperature distribution, and the inserted graph shows the temperature along the z-axis. The laser illumination was from the left to the right in Fig. 5 and the optical axis corresponded to the z-axis. The measurable range of the thermography was 253–1173 K. The temperatures over 1173 K were indicated as 1173 K because the maximum detection temperature of the thermography was 1173 K. The origin of the vertical line corresponds to the center of the temperature over 1173 K. The temperature above 1173 K ( $-0.6 \leq z \leq 0.6 \text{ mm}$ ) corresponded to the area where the glass fiber was generated. To estimate the maximum temperature, a fitting was attempted. The heat source was assumed to be a point, because the laser absorption spot was much smaller than the glass thickness. The temperature distribution of a point heat source on an infinite slab exhibits a Gaussian profile [18]. As a result of Gaussian fitting, the maximum temperature  $T_{\text{max}}$  was calculated to be 1220 K. The softening point of borosilicate glass is 1094 K, so  $T_{\text{max}}$  was higher than the softening

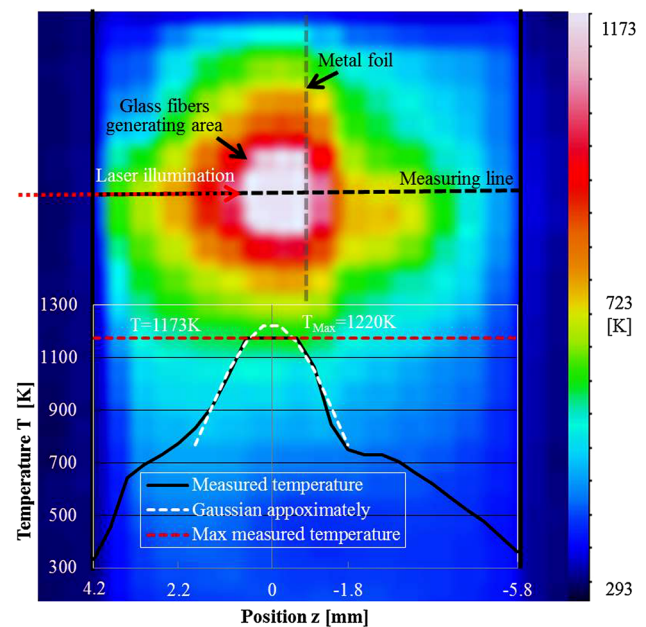


**Fig. 5** Thermal image and temperature graph around the glass fibers generating area. Laser illumination of the sample from the left in the figure heats the sample. *Inserted graph* shows the temperature along the measuring line in the contour, *black line* is the measured temperature by using thermography and the *red line* is the maximum measurable temperature with thermography, 1173 K. The *white line* is the Gaussian fitting of the measured temperature to calculate the maximum temperature of glass during glass fiber generation

point. The borosilicate glass, heated by laser illumination, was sufficiently softened. However,  $T_{\text{max}}$  was lower than the softening point of silica glass (1973 K). Hence, the fibers were generated only from the borosilicate glass. Additionally, the viscosity of the borosilicate glass (at the  $T_{\text{max}}$  area) was  $4.1 \times 10^3 \text{ Pa s}$ . Industrial glass fibers can be produced from softened glass with a viscosity of 50–150 Pa s [12]. Therefore, the viscosity of the glass was higher than that required for industrial glass fibers.

Figure 6 shows the fiber generation mechanism based on the results from SEM images, in situ observation, and the temperature measurement. Figure 6a–e shows the overall view and the upper surface, respectively. The laser illumination heated the metal foil, and the temperature of the side surface of borosilicate glass increased owing to the heat conduction (Fig. 6a). The heated glass absorbed the irradiation, and the fiber fuse phenomenon occurred. The fiber fuse is where the absorbed point heats the surrounding glass and the heat spot moves toward the laser source in the glass fiber [19]. Emission with the same characteristics as observed previously [13–16] was observed. The fiber fuse caused the result that the maximum temperature was measured at  $z = 0 \text{ mm}$ , not at the metal foil ( $z = -0.8 \text{ mm}$ ), as shown in Fig. 5. The volume of the glass increased with increasing temperature. The surface

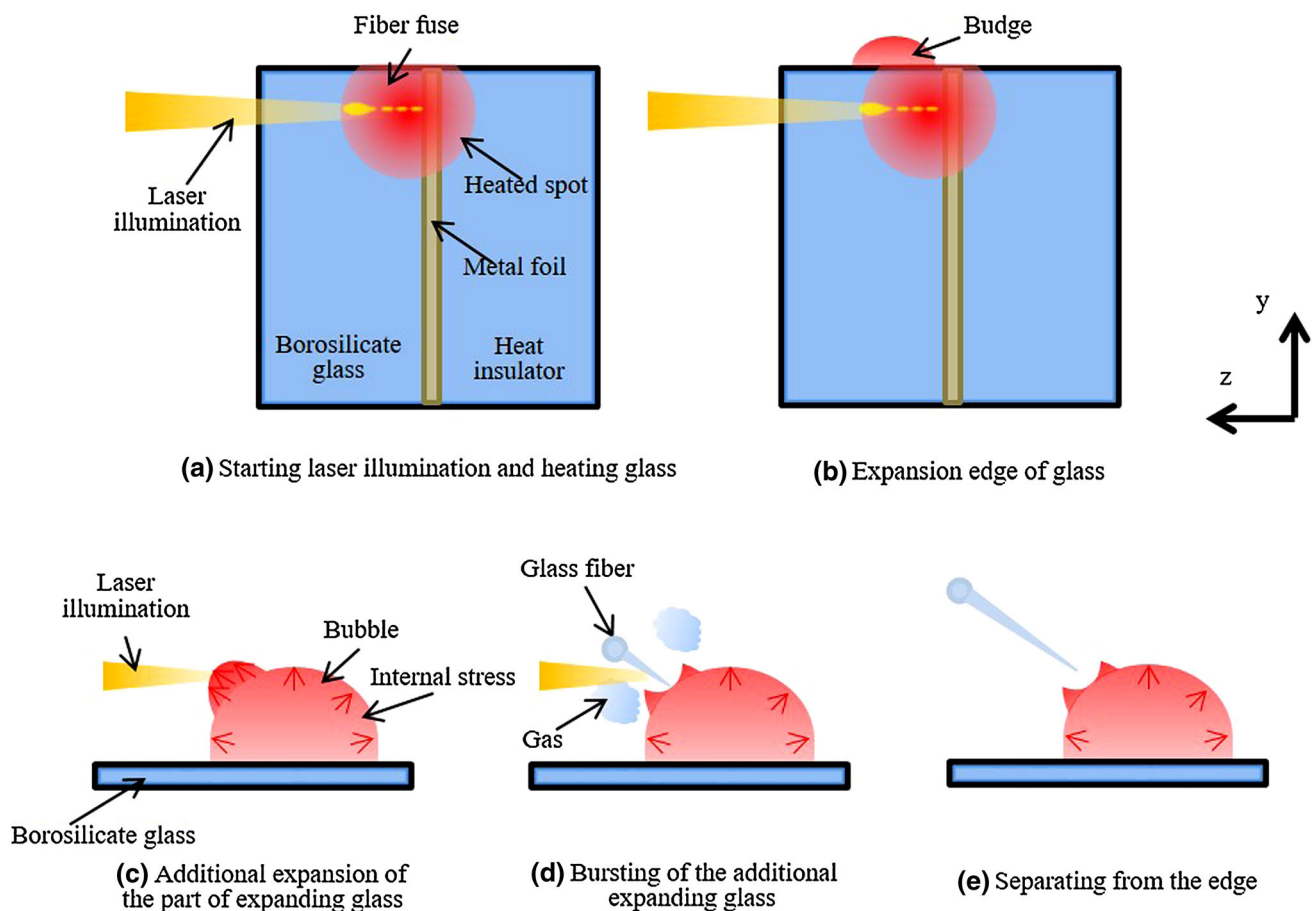


**Fig. 6** Mechanism of generating glass fibers (a, b Macroview, c–e Microview)

became bulged where it was heated, owing to the low viscosity, and formed a convex portion referred to as the bulge (Fig. 6b). Scanning the laser from the original glass to the bulge along the  $y$ -axis direction caused the bubble expansion glass. The borosilicate glass vaporized and the bubble was formed rapidly (Fig. 6c).

Then, the bubble bursts, and the fiber was ejected (Fig. 6d). The temperature was estimated to be  $\sim 1220$  K. In industrial glass fiber formation, a sufficient energy to separate the fiber from the softened glass, which depends on the viscosity and surface tension, is required [12]. The bursting of the bubble caused the fibers to be ejected into the air. Hence, a sufficient energy to separate the fiber was obtained by the bursting. After that, the fibers were separated from the sample (Fig. 6e). The fibers were deposited on the jig/glass slide 3 mm from the generation area.

Nanoparticles were observed on the fiber. The particles were generated from the gas phase or softened glass. Assuming that nanoparticles were formed from gas, the gas was transferred to the glass nanoparticles when the gas was quenched. Air cooling was believed to be sufficiently rapid, because the gas in the microbubble, whose diameter was

$\sim 70$   $\mu\text{m}$ , was ejected into the air (as shown in Fig. 4). In contrast, assuming that the nanoparticles formed from softened glass, the softened glass had to be formed in nanoparticles with a diameter of  $\sim 100$  nm. Moreover, in this case, additional energy should be applied for dispersion; hence, this situation is unlikely during laser ablation. In the case with a femtosecond laser [9], nanoparticles adhered on the glass fibers in the same manner as reported in this paper, and the reason for generating nanoparticles was explained by the cohesion of vaporized glass in the interior of the plasma. Therefore, the gas inside the bubble was also ejected into the air and generated the nanoparticles on the glass fibers (as shown in Fig. 3c).

Although the temperature of the surface was estimated to be  $\sim 1220$  K, glass is indispensable for additional heating for a phase change to gas. The internal temperature of the bulge was higher than the surface temperature of the bubble, because the laser was absorbed in the bulge. Meanwhile, in the case of using a pulsed UV laser [8], nanoparticles were not observed on the glass fibers.

In the case where a short-pulse laser was used, only the glass was illuminated by the laser. In this paper, the laser

irradiation first heated a metal foil. Therefore, the material of the glass fibers may contain metal. Hence, a metal-doped fiber is expected by changing the experimental conditions. Metal doping to the fiber is expected for the application to catalysis, because the fibers possess the feature of a large surface area to volume.

The glass fiber generation requires the heating glass step and the glass emission step. The glass emission step was mainly discussed in this paper. More precise analysis of the heating glass step will reveal the conditions for controlling the volume and diameter of the glass fiber depending on heating time, heating start position and laser power.

#### 4 Conclusions

In summary, we reported a novel glass fiber fabrication technique with a CW laser beam and elucidated the fabrication mechanism. In this technique, the glass fibers possessed the features where the head part was elliptical, the diameter became thinner from the head to the tail, and nanoparticles were attached on the surface. In situ observation showed the fiber generation process. The heated glass became bulged and the bulged area expanded, then shrank, then burst. The bursting ejected glass fibers. The temperature distribution was measured using thermography. As a result, the maximum temperature was estimated to be  $\sim 1220$  K, which was higher than the softening point of borosilicate glass.

**Acknowledgements** Support by the Japan Society for the Promotion of Science under a Grant-in-Aid for Scientific Research (B, 20360065) is gratefully acknowledged.

#### References

1. I. Herszberg, H.C.H. Li, F. Dharmawan, A.P. Mouritz, M. Nguyen, J. Bayandor, *Compos. Struct.* **67**, 205 (2005)
2. J. Paz, J. Díaz, L. Romera, M. Costas, *Compos. Struct.* **133**, 499 (2015)
3. S. Hamid, M.R. Ehsani, *J. Struct. Eng.* **117**, 3417 (1991)
4. M. Kupke, H.P. Wentzel, K. Schulte, *Mat. Res. Innov.* **2**, 164 (1998)
5. Y. Takahashi, T. Mohri, *Eurozoru Kenkyu* **6**, 4 (1991) (**in Japanese**)
6. B. Tan, K. Venkatakrishnan, *Opt. Express* **17**, 1064 (2009)
7. V.N. Tokarev, S. Lazare, C. Belin, D. Debarre, *Appl. Phys. A* **79**, 717 (2004)
8. S. Itoh, M. Sakakura, Y. Shimotsuma, K. Miura, *Appl. Phys. B* **119**, 519 (2015)
9. M. Sivakumar, K. Venkatakrishnan, B. Tan, *Nanoscale Res. Lett.* **4**, 1263 (2009)
10. K. Venkatakrishnan, D. Vipparthy, B. Tan, *Opt. Express* **19**, 15770 (2011)
11. G.A.J. Markillie, H.J. Baker, F.J. Villarreal, D.R. Hall, *Appl. Opt.* **41**, 5660 (2002)
12. M. Yamane, I. Yasui, M. Wada, Y. Kokubu, R. Terai, K. Kondo, S. Ogawa, *Handbook of glass engineering*, 1st edn. (Asakura Publishing Co., Ltd, Japan, 1999), pp. 356–377 (**in Japanese**)
13. H. Hidai, M. Yoshioka, K. Hiromastu, H. Tokura, *Appl. Phys. A* **94**, 869 (2009)
14. H. Hidai, N. Saito, S. Matsusaka, A. Chiba, N. Morita, *Appl. Phys. A* **122**, 4 (2016)
15. S. Itoh, H. Hidai, H. Tokura, *Appl. Phys. A* **112**, 4 (2013)
16. H. Hidai, M. Yoshioka, K. Hiromatsu, H. Tokura, *J. Am. Ceram. Soc.* **93**, 6 (2010)
17. A. Goldsmith, T.E. Waterman, J.J. Hirschhorn, *Handbook of thermophysical properties of solid materials*, vol. 3 (Pergamon Press, New York, 1961), p. 871
18. D. Bäuerle, *Laser processing and chemistry*, 4th edn. (Springer, New York, 2011), p. 21
19. S. Todoroki, *Fiber fuse: light-induced continuous breakdown of silica glass optical fiber* (Springer Japan, Tokyo, 2014), pp. 51–52